Mn_n^- clusters: Size-induced transition to half metallicity

Julius Jellinek,[1,*] Paulo H. Acioli,[1,†] Juan Garciá-Rodeja,[1,‡] Weijun Zheng,[2] Owen C. Thomas,[2] and Kit H. Bowen, Jr.[2]
[1]*Chemistry Division, Argonne National Laboratory, Argonne, Illinois 60439, USA*
[2]*Departments of Chemistry and Materials Science, Johns Hopkins University, Baltimore, Maryland 21218, USA*
(Received 29 April 2005; revised manuscript received 3 August 2006; published 3 October 2006)

Results of a theoretical and experimental photoelectron spectroscopy (PES) study of the size evolution of electronic properties of small Mn_n^- clusters are presented. The agreement between the computed and measured data verifies the validity of the theoretical treatment. The theoretical analysis leads to the first prediction of nanoscale half metallicity and the size-induced transition to it. It also points to the type of experiments (spin-polarized PES) that will be able to directly verify the predicted phenomenon.

DOI: 10.1103/PhysRevB.74.153401 PACS number(s): 36.40.−c, 31.15.Ew, 33.60.−q, 71.30.+h

The changes in electronic features, in general, and the transition to metallicity, in particular, are among the most intricate and intriguing aspects of the size evolution of properties of metal clusters, or, more precisely, atomic clusters of elements that are metals in bulk quantities.[1] To identify a size-induced transition to metallicity one could use different characteristic attributes, which include transport properties, electronic features, as well as dielectric and magnetic characteristics. The answer to the question "at what size does a cluster of a metallic element become a metal?" and the details of the transition to metallicity depend on the property used to probe and gauge the transition. Driven primarily by experimental considerations, the attribute utilized most often so far is the electronic structure of the clusters as a function of their size. It has been used to study the transition to metallicity in mercury[2–6] and, more recently, magnesium[7–10] clusters.

Here we present results of a combined theoretical/experimental investigation of the size evolution of the electronic properties of Mn_n^- clusters. The theoretical analysis points to what can be viewed as the first evidence of a finite-size analog of the half metallic state. Bulk half metals—systems with spin-polarized conductivity—are the subject of intense research activity.[11] The finite-size analog(s) of bulk half metallicity, however, remains *terra incognita*. Understanding this analog(s) and the transition to it (them) is central to many areas of nanoscience and nanotechnology, especially those where spin-polarized processes, including transport, could lead to principally new phenomena and, consequently, applications.[12]

The central subject of our interest is the spectra of electron binding energies (EBE) in Mn_n^- as a function of n. Computationally, we obtained these spectra by combining gradient-corrected density functional theory (DFT) with a new highly accurate scheme for conversion of the Kohn-Sham eigenenergies into EBE.[13] We used the B3LYP exchange-correlation functional and the Stuttgart pseudopotential with its corresponding basis set[14] as implemented in the *Gaussian 98* package.[15] The choice of the functional was based on tests performed with a variety of alternatives (B3LYP, BLYP, BP86, BPW91, B3PW91, and PBE) using all-electron computations with the 6-311+G* basis set. Available experimental and high-quality computational data on neutral and charged Mn_n, $n=1-2$, served as a basis for evaluation. The selection of the Stuttgart pseudopotential was made based on comparisons with the results of the all-electron computations. Because of the open-shell nature of Mn, the unrestricted formalism was employed.

The equilibrium structural forms (isomers) of the clusters were obtained through unconstrained gradient-driven optimizations. For each cluster size, a variety of different initial guess configurations were considered, and for each configuration different spin states were studied. For each total spin, different implementations were explored, including broken symmetry ones. Normal mode analysis was applied to the stationary configurations obtained to distinguish true isomers from transition state conformations.

Experimentally, the EBE were measured using photoelectron detachment spectroscopy, which was conducted by crossing a mass-selected beam of negative ions with a fixed-frequency photon beam and energy-analyzing the resultant photodetached electrons. The EBE were determined from the relationship $h\nu$=EBE+EKE, where $h\nu$ is the photon energy and EKE is the measured electron kinetic energy. The apparatus—a pulsed, anion photoelectron spectrometer—consists of a laser vaporization source, a linear time-of-flight mass selector, a mass gate, a momentum decelerator, a Nd:YAG photodetachment laser, and a magnetic bottle electron energy analyzer. The Mn_n^- clusters were generated by ablating a rotating and translating manganese rod with 2.33 eV/photon laser pulses from a second Nd:YAG laser, while a synchronized pulsed valve delivered helium gas from a 4 atm reservoir. Photodetachment was accomplished with 3.493 eV photons. All photoelectron spectra were calibrated against the atomic transitions of the copper anion. Cooling studies, conducted by varying the helium pressure, suggest 300 ± 100 K as an estimate for the temperature of the Mn_n^- clusters.

Figure 1 shows the lowest energy structures and their binding energies for neutral and anionic Mn_n, $n=2-8$, as obtained in our computations. Since the Mn^- anion is unstable, the binding energies of both the neutral and the anionic Mn_n are referred to the energies of n neutral Mn atoms; for the anions this definition translates into the sum of the binding energy of the extra electron in Mn_n^- and the binding energy of the neutral Mn_n. As is clear from the figure, the strength of bonding increases with n, with the value of the binding energy per atom in Mn_8 approaching 18% of the cohesive energy of bulk α manganese (2.92 eV).[16] The antiferromagnetic (0 μ_B) and ferromagnetic (10 μ_B) states of

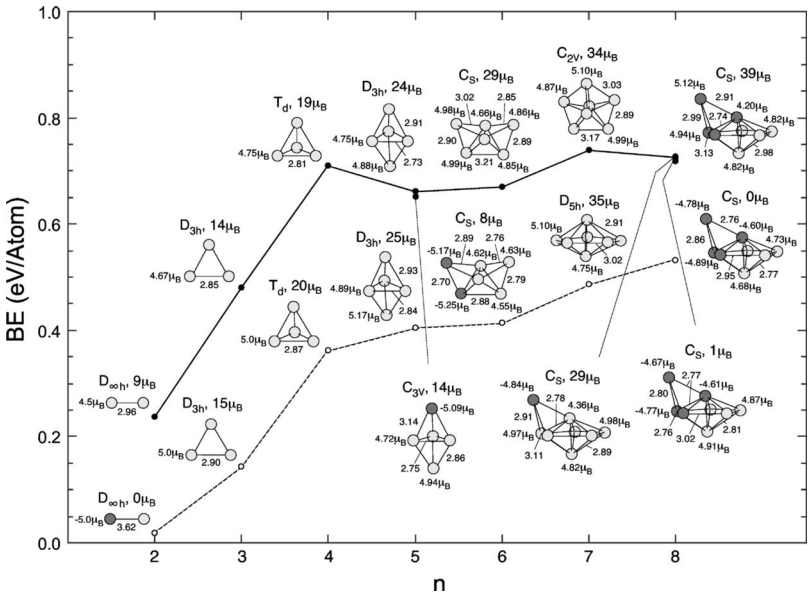

FIG. 1. Most stable structures ("Iso 1") and their binding energies per atom, symmetries, and total and atomic magnetic moments for neutral (open circles) and anionic (full circles) Mn_n, $n=2-8$. The interatomic distances are in Å. Light shading of the atoms indicates majority (α) spin, dark shading, minority (β) spin. For Mn_5^- and Mn_8^-, we also show energetically close isomers ("Iso 2," and "Iso 2" and "Iso 3," respectively).

Mn_2 are competitive, with the former winning by 0.002 eV/atom. Results of earlier computational studies[17] vary as to which of the two is more stable. Experiments[18] point to the antiferromagnetic state as the energetically more favorable.

With the exception of the $n=7$ case, the packing and the symmetry of the most stable forms of the neutral and anionic clusters are the same, with the neutrals having slightly larger bond lengths. Attaching an electron to Mn_7 lowers its preferred D_{5h} symmetry to the C_{2v} symmetry of the favored structure of Mn_7^-. The total magnetic moment of the lowest energy states of Mn_n, $n=3-5$ and 7, arises from ferromagnetic ordering of the moments of the individual atoms, which are close to 5 μ_B—the value characteristic of a free Mn atom. The preferred total magnetic moment of Mn_6 is 8 μ_B. It is a consequence of a ferrimagnetic ordering, with spins of two atoms antiparallel to spins of four atoms. The most favored, zero total magnetic moment of Mn_8 arises from antiferromagnetic ordering of the atomic spins in this cluster.

In all anionic Mn_n^-, $n=2-8$, the energetically preferred value of the total magnetic moment is a consequence of ferromagnetic ordering of the spins of all the atoms, with the extra electron joining the minority spin manifold. The latter can be rationalized by taking into account that in each Mn atom in its ground ($[Ar]3d^54s^2$) state all five electrons of the half filled d shell belong to the majority manifold. These electrons form a filled α subshell of the atomic d shell and, because of the ferromagnetic ordering of the atomic spins in the cluster, give rise to what is, at least qualitatively, a filled "α subband" of the cluster "d band."

For Mn_5^- and Mn_8^- we have found structures and states with energies very close to those of the corresponding most stable isomers. These are also shown in Fig. 1. A C_{3v} structure of Mn_5^- with total spin of 14 μ_B is only 0.007 eV/atom less stable than its lowest energy D_{3h} isomer. For Mn_8^-, two structures, both of C_s symmetry, with magnetic moments of 29 μ_B and 1 μ_B, are only 0.002 eV/atom and 0.007 eV/atom, respectively, higher in energy than its most stable isomer with magnetic moment of 39 μ_B.

The structures and states described above show both agreement with and deviation from the findings of earlier computational[19–21] and experimental[22] studies. These earlier studies were done almost exclusively on neutral Mn_n. Since the focus of this report is on the size evolution of the electronic properties of anionic Mn_n^-, we defer further discussion of the details to a future publication. Here we note only that the major reason for the discrepancy in the different DFT-based results is the choice of the exchange-correlation functional; as indicated above, our choice of this functional is based on extensive and careful tests. An additional point that has to be taken into account when comparing computed moments with data derived from magnetic deflection experiments is that these data necessarily invoke models (e.g., the superparamagnetic model). These models may and, indeed, do affect the outcome. In contrast, photoelectron spectroscopy measurements provide high-accuracy data that can be compared directly with the results of computations. An agreement between the computed and measured EBE for a variety of different systems (e.g., clusters of different sizes, cf. Refs. 8–10, 23, and 24) serves as a validation of the computational framework used.

Figure 2 shows the EBE spectra computed and measured for Mn_n^-, $n=3-8$. For all sizes, the spectrum computed for the most stable configuration of the cluster is displayed. For Mn_5^- and Mn_8^-, the spectra computed for the first and the first and second energetically close isomers, respectively, are shown as well. The computed and measured data display a good agreement. Not only do they span the same energy segments, but they also exhibit the same patterns. As illustrated by the cases of Mn_5^- and Mn_8^-, the agreement becomes only better when one considers the possible contributions of higher energy isomers. In fact, examination of the shapes of the measured spectra for clusters of other sizes lends support to the conjecture that they also include contributions from higher energy isomers.

The quantity of special interest is the difference (gap) between the binding energies of the most external (HOMO) and next to it (HOMO-1) electrons in Mn_n^- as a function of n.

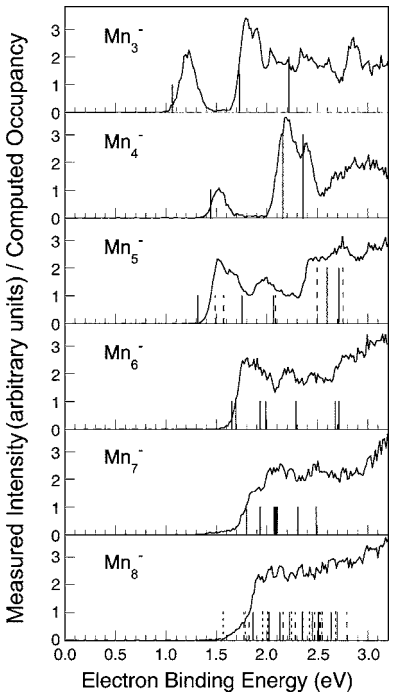

FIG. 2. Computed (vertical bars) and measured (graphs) EBE spectra. For each cluster size, the solid bars correspond to the most stable conformation. For Mn_5^- and Mn_8^-, the long-dashed and short-dashed bars represent the first and second, respectively, energetically close isomers (cf., Fig. 1).

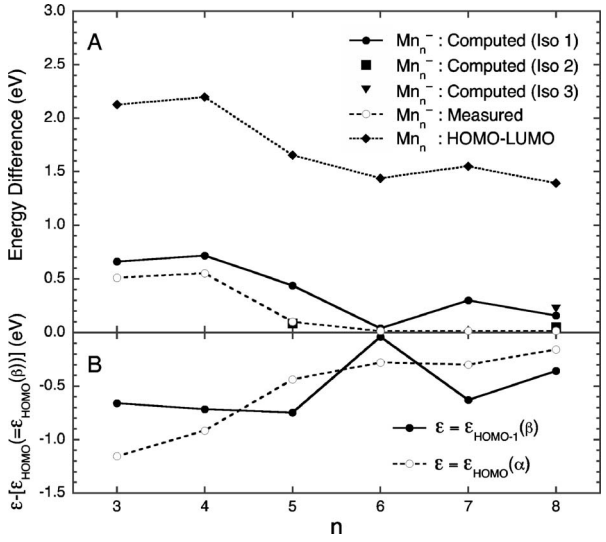

FIG. 3. Panel A: Computed (solid line and individual squares and triangles) and experimentally derived (dashed line) difference between the binding energies of the two most external electrons in Mn_n^- as a function of n. The computed results are for the isomers of Mn_n^- shown in Fig. 1 The experimental error estimate is ±0.15 eV. The dotted line is the HOMO-LUMO gap computed for the most stable isomers of Mn_n. Panel B: Computed difference between the eigenenergies of the α electron and β electron, respectively, closest to the HOMO electron, and the eigenenergy of the HOMO electron in the most stable isomer of Mn_n^- as a function of n.

As discussed in Refs. 9, 10, and 24, this difference is the *anionic* finite-size analog of the gap between the valence and the conduction bands in bulk conductors, and it has been used to analyze the phenomenon of size-induced transition to metallicity in Mg_n^- clusters.[8–10,24] In panel A of Fig. 3 we present the graphs of this difference for Mn_n^-, $n=3-8$, as obtained in our computations and measurements. The experimental values are obtained from the positions of the first two (possibly overlapping) peaks in the graphs of Fig. 2 using the methodology described in Ref. 8. As mentioned, different isomers may contribute to these peaks, and this has to be taken into account when evaluating and interpreting the gaps derived from the measurements. As seen in panel A of Fig. 3, it is isomers 2 of Mn_5^- and of Mn_8^- that are responsible for and explain the experimental values of the gap in these clusters.

The graphs in panel *A* also show that both the computations and the measurements indicate a decrease, albeit not monotonic, in the HOMO/(HOMO-1) EBE gap as n increases, and its closure at $n=6$. A detailed understanding of the meaning of this gap closure (it is usually viewed as an indication of transition to a finite-size analog of a metallic state) is provided by the two graphs in panel B of Fig. 3. These depict the size dependence of the difference between (a) the eigenenergy of the HOMO electron in the majority (α) spin manifold and (b) the HOMO-1 electron in the minority (β) spin manifold, on the one hand, and the eigenenergy of the HOMO electron of the cluster, which for all n belongs to the β manifold, on the other. Inspection of the graphs reveals that the gap closure at $n=6$ has a spin-polarized character: There is closure in terms of the eigenenergies of the β electrons (the energy difference is 0.004 eV), but the gap between the energies of the HOMO electron and the most external α electron remains large (0.279 eV) as evaluated by a relevant energy gauge (e.g., the value of kT at room temperature, 0.03 eV). This feature can be viewed as a finite-size analog of the bulk *half metallic* state, the signature attribute of which is nonzero value of the density of states (DOS) (or, alternatively, zero gap in this density) across the Fermi level as evaluated in terms of the states corresponding to one spin manifold, and zero value of the DOS (or, alternatively, finite gap) as evaluated in terms of the states corresponding to the other spin manifold. The above analysis represents the identification of the phenomenon of finite-size half metallicity and is a theoretical prediction. A way to verify and confirm this phenomenon experimentally is to perform spin-polarized electron photodetachment measurements, which will target electrons with a given spin and/or will evaluate not only the kinetic energy, but also the spin of the photodetached electrons.

The size-induced transition to half metallicity as analyzed in terms of the graphs of Fig. 3 describes the phenomenon as it exhibits itself in *anionic* clusters. To stress this point, in panel A of Fig. 3 we also show the HOMO-LUMO gap as computed in the most stable structures of the neutral Mn_n (this gap is often invoked as the analog of the bulk band gap in *neutral* finite systems). As is clear from the graphs of panel A, the experiments indeed probe the electronic properties of the anionic Mn_n^-, and the gap closure takes place in Mn_6^-, not Mn_6. Moreover, as analyzed in terms of the graphs in panel B of Fig. 3, it is specific to the lowest energy isomer of Mn_6^-. Since the electronic properties of clusters (more gen-

erally, finite systems) change with their isomeric form and charge state, other types of transitions, or the same transition but at a different size, may characterize the same clusters dependently on the choice of their structure(s) and/or total charge. In fact, the isomeric forms and their energy ordering themselves may be, and in the small size range usually are, functions of the charge state. Thus the charge has a direct and indirect effect on the size evolution of the electronic properties, in general, and the finite-size analogs of the transition to metallicity or half metallicity, in particular. The different manifestations of these size-induced transitions, corresponding to different structural forms and/or charge states, represent different facets of phenomena that are considerably more intricate and complex than their bulk-limit analogs. The different facets may have to be combined in the analyses and interpretation of the experimental data. For example, as illustrated above through the cases of Mn_5^- and Mn_8^-, one may have to invoke more than one isomeric form of the clusters dependently on the experimental conditions (e.g., temperature or rate of cooling).

In summary, in this paper we described and analyzed computational and experimental results on the size evolution of the electronic properties of small Mn_n^- clusters and presented theoretical/computational evidence for the finite-size analog of the half metallic state and the transition to it. Spin-polarized photoelectron spectroscopy techniques for clusters will have to be developed and applied for experimental verification and corroboration of the concept of finite-size half metallicity. Future studies will have to include further development of the conceptual framework and extensions to clusters of larger sizes.

Note added in proof. Recently, an additional paper on neutral Mn_n clusters has been published.[25]

This work was supported by the Office of Basic Energy Sciences, Division of Chemical Sciences, Geosciences, and Biosciences, U.S. Department of Energy, under Contract No. W-31-109-Eng-38 (J.J., P.H.A., and J.G.R.), and Division of Materials Science and Engineering, under Grant No. DE-FG02-95ER45538 (K.H.B.). Acknowledgement is also made to PRF, Grant No. 28452-AC6 (K.H.B.), and to Diputación de la Coruña and CESGA (J.G.R.) for partial support.

*Corresponding author. Email address: jellinek@anl.gov
†Permanent address: Department of Physics, Northeastern Illinois University, Chicago, IL 60625.
‡Present address: Departamento de Fisica de la Materia Condensada, Facultad de Fisica, Universidad de Santiago de Compostela, E-15782 Santiago de Compostela, Spain.

[1] B. von Issendorff and O. Cheshnovsky, Annu. Rev. Phys. Chem. **56**, 549 (2005), and references therein.
[2] K. Rademann, B. Kaiser, U. Even, and F. Hensel, Phys. Rev. Lett. **59**, 2319 (1987).
[3] C. Brechignac, M. Broyer, Ph. Cahuzac, G. Delacretaz, P. Labastie, J. P. Wolf, and L. Woste, Phys. Rev. Lett. **60**, 275 (1988).
[4] M. E. Garcia, G. M. Pastor, and K. H. Bennemann, Phys. Rev. Lett. **67**, 1142 (1991).
[5] H. Haberland, B. von Issendorf, Y. Yufeng, and T. Kolar, Phys. Rev. Lett. **69**, 3212 (1992).
[6] R. Busani, M. Folkers, and O. Cheshnovsky, Phys. Rev. Lett. **81**, 3836 (1998).
[7] T. Diederich, T. Doppner, J. Braune, J. Tiggesbaumker, and K.-H. Meiwes-Broer, Phys. Rev. Lett. **86**, 4807 (2001).
[8] O. C. Thomas, W. Zheng, S. Xu, and K. H. Bowen, Phys. Rev. Lett. **89**, 213403 (2002).
[9] P. H. Acioli and J. Jellinek, Phys. Rev. Lett. **89**, 213402 (2002).
[10] J. Jellinek and P. H. Acioli, J. Phys. Chem. A **106**, 10919 (2002); **107**, 1670 (2003).
[11] P. A. Dowben and R. Shomski, J. Appl. Phys. **95**, 7453 (2004), and references therein.
[12] S. A. Wolf, D. D. Awschalom, R. A. Buhrman, J. M. Daughton, S. von Molnár, M. L. Roukes, A. Y. Chtchelkanova, and D. M. Treger, Science **294**, 1488 (2001).
[13] J. Jellinek and P. H. Acioli, J. Chem. Phys. **118**, 7783 (2003).
[14] M. Dolg, U. Wedig, H. Stoll, and H. Preuss, J. Chem. Phys. **86**, 866 (1987).
[15] M. J. Frisch, G. W. Trucks, H. B. Schlegel, G. E. Scuseria, M. A. Robb, J. R. Cheeseman, V. G. Zakrzewski, J. A. Montgomery, Jr., R. E. Stratmann, J. C. Burant, S. Dapprich, J. M. Millam, A. D. Daniels, K. N. Kudin, M. C. Strain, O. Farkas, J. Tomasi, V. Barone, M. Cossi, R. Cammi, B. Mennucci, C. Pomelli, C. Adamo, S. Clifford, J. Ochterski, G. A. Petersson, P. Y. Ayala, Q. Cui, K. Morokuma, P. Salvador, J. J. Dannenberg, D. K. Malick, A. D. Rabuck, K. Raghavachari, J. B. Foresman, J. Cioslowski, J. V. Ortiz, A. G. Baboul, B. B. Stefanov, G. Liu, A. Liashenko, P. Piskorz, I. Komaromi, R. Gomperts, R. L. Martin, D. J. Fox, T. Keith, M. A. Al-Laham, C. Y. Peng, A. Nanayakkara, M. Challacombe, P. M. W. Gill, B. Johnson, W. Chen, M. W. Wong, J. L. Andres, C. Gonzalez, M. Head-Gordon, E. S. Replogle, and J. A. Pople, *Gaussian 98* (Gaussian, Inc. Pittsburgh, PA, 1998).
[16] C. Kittel, *Introduction to Solid State Physics*, (Wiley, New York, 1986), 6th ed.
[17] B. Wang and Z. Chen, Chem. Phys. Lett. **387**, 395 (2004), and references therein.
[18] R. van Zee, C. A. Baumann, and W. Weltner, Jr., J. Chem. Phys. **74**, 6977 (1981).
[19] S. K. Nayak, M. Nooijen, and P. Jena, J. Phys. Chem. A **103**, 9853 (1999).
[20] N. O. Jones, S. N. Khanna, T. Baruah, and M. R. Pederson, Phys. Rev. B **70**, 045416 (2004).
[21] P. Bobadova-Parvanova, K. A. Jackson, S. Srinivas, and M. Horoi, J. Chem. Phys. **122**, 014310 (2005).
[22] M. B. Knickelbein, Phys. Rev. B **70**, 014424 (2004), and references therein.
[23] P. H. Acioli and J. Jellinek, Eur. Phys. J. D **24**, 27 (2003).
[24] J. Jellinek and P. H. Acioli, *in Metal-Ligand Interaction in Molecular-, Nano- and Macro-Systems in Complex Environments*, edited by N. Russo, D. R. Salahub, and M. Witko (Kluwer, Dordrecht, 2003), p. 121.
[25] M. Kabir, A. Mookerjee, and D. G. Kanhere, Phys. Rev. B **73**, 224439 (2006).